



Cite this: *Food Funct.*, 2017, **8**, 2601

An inhibition mechanism of dihydromyricetin on tyrosinase and the joint effects of vitamins B₆, D₃ or E

Meihui Fan,^a Guowen Zhang, ^{*a} Junhui Pan^a and Deming Gong^b

Dihydromyricetin (DMY), a natural flavonoid, was found to effectively inhibit tyrosinase activity in a mixed-type manner with an IC₅₀ value of $(3.66 \pm 0.14) \times 10^{-5}$ mol L⁻¹. DMY combined with the dietary vitamin D₃ at lower concentrations exhibited a synergistic effect on the inhibition of tyrosinase. The formation of a DMY–tyrosinase complex led to fluorescence quenching and conformational changes of tyrosinase, which was driven mainly by hydrophobic interactions and hydrogen bonds. The molecular simulation further found that DMY inserted into the active pocket of tyrosinase interacted with amino acid residues Tyr78, His85, and Ala323, occupying the catalytic center of tyrosinase to hinder entrance of the substrate, leading to the inhibition of tyrosinase. This study may provide a scientific foundation for screening effective tyrosinase inhibitors.

Received 13th February 2017,
Accepted 19th June 2017

DOI: 10.1039/c7fo00236j

rsc.li/food-function

1. Introduction

Tyrosinase belongs to the type 3 copper protein family containing dinuclear copper ions and widely exists in animals.¹ It is a critical enzyme in the synthesis process of melanin pigments, catalyzing *ortho*-hydroxylation of monophenols to *o*-diphenols and then to corresponding *o*-quinones.² Its overexpression may lead to several pigmentation disorders, such as age spots, freckles, melasma, and malignant melanoma. Therefore, the study of tyrosinase inhibitors is of great significance in the treatment of some pigmentation disorders.

Currently, some known tyrosinase inhibitors have been reported to have some side effects.³ For instance, kojic acid, hydroquinone, and corticosteroids are used as tyrosinase inhibitors in the cosmetic industry, but some studies show they can give rise to dermatitis, skin irritation, melanocyte destruction, cytotoxicity, and skin cancer.⁴ Natural plants rich in bioactive chemicals are attracting researchers' attention in screening for new candidates.^{5,6} Apigenin was found to inhibit polyphenol-oxidase activity reversibly in a mixed-type manner with an IC₅₀ of 3.92×10^{-5} mol L⁻¹.⁷ Glabridin was reported to inhibit the activity of tyrosinase in a noncompetitive manner with an IC₅₀ of 4.3×10^{-7} mol L⁻¹.⁸ Avocado proanthocyanidins inhibited tyrosinase in a reversible and competitive manner.²

Dihydromyricetin (DMY, structure shown in Fig. 1A), also known as ampelopsin, exists in many edible and medicinal plants, such as *Hovenia dulcis* Thumb and *A. grossedentata*. It has shown many curative effects, including decreasing blood pressure, reducing blood sugar, inhibiting hypertension, and protecting the liver.^{9,10} DMY was reported to be an effective candidate for the treatment of alcohol caused disorders.¹¹ It was found that DMY can effectively inhibit the activity of tyrosinase.¹² However, the study was restricted to the enzymatic activity assay, and the inhibitory mechanism of DMY on tyrosinase is unknown. Therefore, investigating the inhibition mechanism of DMY on tyrosinase may provide valuable information for the functional applications of DMY as a tyrosinase inhibitor. In addition, vitamins B₆, D₃, and E (structures shown in Fig. 1B) are essential vitamins for human body. These vitamins and DMY can be obtained from daily dietary, and they may coexist in the human body. Therefore, it is also necessary to study the joint inhibitory effects of DMY and vitamins B₆, D₃, or E on tyrosinase activity.

The main objectives of this study were to investigate the inhibitory kinetics, binding characteristics and inhibitory mechanisms of DMY on tyrosinase, and to determine the joint effects of vitamins B₆, D₃, or E on DMY inhibiting tyrosinase by a combination of UV–Vis absorption, fluorescence, circular dichroism (CD), Fourier transform infrared (FT–IR), and molecular docking approaches. This study is expected to benefit further understanding of the inhibitory mechanism of DMY on tyrosinase and provide a scientific foundation for screening effective tyrosinase inhibitors.

^aState Key Laboratory of Food Science and Technology, Nanchang University, 235 Nanjing East Road, Nanchang 330047, China. E-mail: gwzhang@ncu.edu.cn; Fax: +86-791-88304347; Tel: +86-791-88305234

^bNew Zealand Institute of Natural Medicine Research, 8 Ha Crescent, Auckland 2104, New Zealand

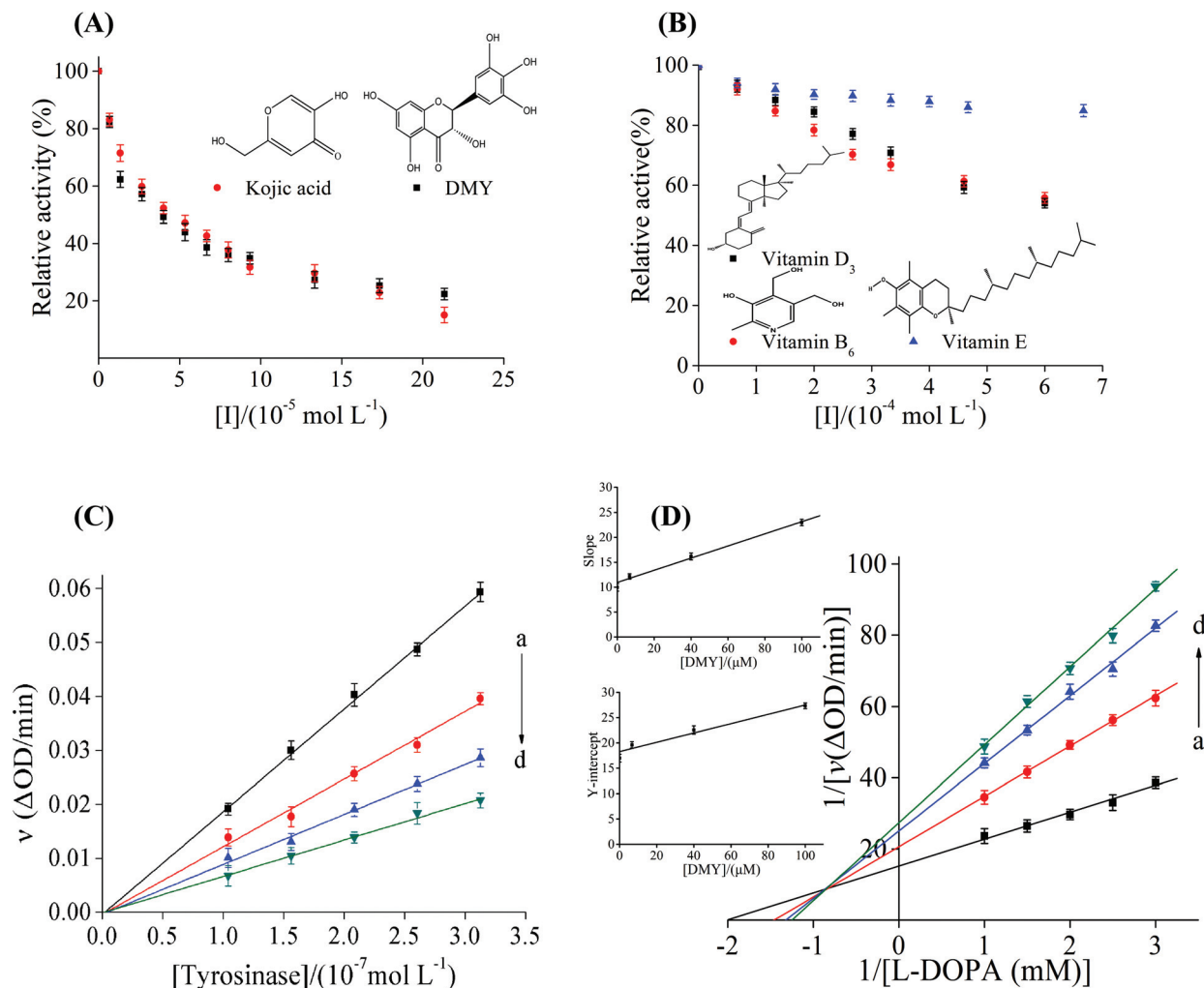


Fig. 1 (A) Inhibitory effects of DMY and kojic acid on tyrosinase (pH 6.8, $T = 303$ K). $c(\text{tyrosinase}) = 2.08 \times 10^{-7} \text{ mol L}^{-1}$, and $c(\text{L-dopa}) = 5.0 \times 10^{-4} \text{ mol L}^{-1}$. (B) Inhibitory effects of vitamins B₆, D₃, or E on tyrosinase, respectively. $c(\text{vitamin B}_6) = 0\text{--}6.67 \times 10^{-4} \text{ mol L}^{-1}$, $c(\text{vitamin D}_3)$ and $c(\text{vitamin E}) = 0\text{--}6.0 \times 10^{-4} \text{ mol L}^{-1}$. (C) Plots of the v versus [tyrosinase]. $c(\text{L-dopa}) = 5.0 \times 10^{-4} \text{ mol L}^{-1}$, and $c(\text{DMY}) = 0, 0.67, 4.0, \text{ and } 10.0 \times 10^{-5} \text{ mol L}^{-1}$ for curves a \rightarrow d, respectively. (D) Lineweaver-Burk plots. $c(\text{tyrosinase}) = 2.08 \times 10^{-7} \text{ mol L}^{-1}$, $c(\text{DMY}) = 0, 0.67, 4.0, 10.0 \times 10^{-5} \text{ mol L}^{-1}$ for curves a \rightarrow d, respectively. The secondary replots of slope versus [tyrosinase] and Y-intercept versus [tyrosinase] are in the inset.

2. Materials and methods

2.1. Chemicals and materials

Tyrosinase (EC 1.14.18.1, 128 kDa) was purchased from Worthington Biochemical Co., and its stock solution ($1.56 \times 10^{-5} \text{ mol L}^{-1}$) was prepared in 0.05 mol L^{-1} sodium phosphate buffer (pH 6.8). DMY (purity $\geq 98\%$), vitamins B₆ (purity $\geq 98\%$), D₃ (purity $\geq 99.8\%$), and E (purity $\geq 98\%$), and L-dopa (purity $\geq 99\%$) were obtained from Aladdin Chemical Co. (Shanghai, China). The stock solutions of DMY ($4.0 \times 10^{-3} \text{ mol L}^{-1}$), vitamin D₃ ($1.0 \times 10^{-2} \text{ mol L}^{-1}$), and vitamin E ($1.0 \times 10^{-2} \text{ mol L}^{-1}$) were made in dimethyl sulfoxide (DMSO) and then to a specified volume by adding sodium phosphate buffer (pH 6.8). In the whole process of the experiment, the content of DMSO was kept below 3.33%.¹³ The stock solutions of vitamin B₆ ($2.0 \times 10^{-2} \text{ mol L}^{-1}$) and L-dopa ($5.0 \times 10^{-3} \text{ mol L}^{-1}$) were made in the buffer solution. All the stock solutions were

stored at 4°C , and all reagents and solvents were of analytical purity grade. Fresh ultra-purified water was used throughout the whole study.

2.2. Tyrosinase activity assay

The enzyme activity assay was performed on an UV-Vis spectrophotometer (Persee TU-1901, Beijing, China) based on our previous method with slight modification.¹⁴ In a 3.0 mL reaction system, a series of different inhibitors (DMY, vitamins B₆, D₃, or E) and a fixed concentration of tyrosinase ($2.08 \times 10^{-7} \text{ mol L}^{-1}$) were incubated for 1 h at 30°C . L-Dopa ($5.0 \times 10^{-4} \text{ mol L}^{-1}$) was added to the complex solution to initiate the reaction and then absorbance at 475 nm of the mixture was determined every 5 s. Kojic acid was used as a positive control. The enzyme activity was calculated by the following relationship: relative activity of tyrosinase (%) = (slope of reaction kinetics equation obtained by reaction with inhibitor)/

(slope of reaction kinetics equation obtained by reaction without inhibitor) $\times 100\%$.^{15,16}

2.3. Kinetic analysis

The mixed-type inhibition mechanism can be analyzed on the basis of the Lineweaver–Burk equation in a double reciprocal form as follows:¹⁷

$$\frac{1}{\nu} = \frac{K_m}{V_{\max}} \left(1 + \frac{[I]}{K_i} \right) \frac{1}{[S]} + \frac{1}{V_{\max}} \left(1 + \frac{[I]}{K_{is}} \right) \quad (1)$$

where ν is the enzyme reaction velocity in the absence and presence of DMY, K_m denotes the Michaelis–Menten constant; $[I]$ and $[S]$ are the concentrations of DMY and L-dopa, respectively; K_i is the constant of the DMY binding with free tyrosinase, and K_{is} represents the constant of DMY binding to the L-dopa–tyrosinase complex. Secondary plots were plotted from:¹⁸

$$\text{Slope} = \frac{K_m}{V_{\max}} + \frac{K_m[I]}{V_{\max}K_i} \quad (2)$$

$$\text{Y-intercept} = \frac{1}{V_{\max}^{\text{app}}} = \frac{1}{V_{\max}} + \frac{1}{K_{is}V_{\max}}[I] \quad (3)$$

2.4. Fluorescence titration experiments

According to our previous method,¹⁴ the fluorescence spectra were measured on a spectrofluorophotometer (Model F-7000, Hitachi, Japan) equipped with a thermostat bath. A 2.5 mL sample of tyrosinase solution (2.4×10^{-6} mol L⁻¹) was added to the 1.0 cm path-length quartz cell and then the solution was titrated by different concentrations of DMY solution ($0\text{--}32 \times 10^{-6}$ mol L⁻¹). All of the mixtures were kept for 5 min to equilibrate, and then the fluorescence emission spectra were recorded at 298, 304, and 310 K from 290 to 500 nm by excitation at 280 nm. The emission and excitation bandwidths were both set at 2.5 nm. To correct the fluorescence background, the fluorescence spectra of sodium phosphate buffer (pH 6.8) were deduced.

Synchronous fluorescence spectra were measured from 200 to 400 nm by scanning the excitation wavelength and emission wavelength interval ($\Delta\lambda$) at 15 and 60 nm.

In consideration of the re-absorption and inner filter, the fluorescence data were corrected according to the following relationship:¹⁹

$$F_c = F_m e^{(A_1 + A_2)/2} \quad (4)$$

where F_c and F_m are the corrected and measured fluorescence, A_1 and A_2 indicate the absorbance of DMY at excitation and emission wavelengths, respectively.

A Red edge excitation shift (REES) of free tyrosinase was compared to that of the DMY–tyrosinase complex. DMY solutions with various concentrations ($0\text{--}32 \times 10^{-6}$ mol L⁻¹) were added into the tyrosinase solution (2.4×10^{-6} mol L⁻¹), then the fluorescence emission spectra were recorded at different excitation wavelengths ranging from 280 to 300 nm with 4 nm increment.

2.5. CD spectra study

CD measurements (190–250 nm) of tyrosinase with increasing concentrations of DMY were conducted on a CD spectrometer (MOS 450, Bio-Logic, Claix, France) equipped with a quartz cell of 1.0 mm optical path length under constant nitrogen flush at room temperature. The concentration of tyrosinase was 2.4×10^{-6} mol L⁻¹, and the molar ratios of DMY to tyrosinase varied as 0 : 1, 1 : 8, and 1 : 4, respectively. All CD spectra were corrected by removing the buffer signal. The online SELCON3 program was used to calculate the contents of different secondary structures of tyrosinase with CD spectra data (<http://dichroweb.cryst.bbk.ac.uk/html/home.shtml>).²⁰

2.6. FT-IR spectra measurements

FT-IR spectra were scanned using a FT-IR spectrometer (Thermo Nicolet-5700, USA) *via* the germanium attenuated total reflection (ATR) method with a resolution of 4 cm⁻¹ and 32 scans. The spectra of tyrosinase (2.4×10^{-6} mol L⁻¹) in the absence and presence of DMY (0.6×10^{-6} mol L⁻¹) were measured in the range of 1800–1400 cm⁻¹. The absorbance data about free DMY and buffer solutions were obtained and deducted. Then the FT-IR spectra and curve-fitted results of an amide I band were used to analyze the secondary structure compositions of tyrosinase and its DMY complex by utilizing Omnic software (version 7.2, Nicolet Instrument Co, Madison, WI, USA).

2.7. Molecular docking

The probable interaction between tyrosinase and DMY was further analyzed by the docking program (AutoDock 4.2, Scripps, USA). The 3D structure of DMY was constructed in Chem3D Ultra 8.0 and the X-ray crystal structure of *Agaricus bisporus* tyrosinase was retrieved from PDB data base (ID: 2Y9X). The dimension grid box (90 Å \times 90 Å \times 102 Å) and the grid spacing of 0.619 Å were defined to enclose the active site. In the preparation of molecule docking, the entire water molecules in tyrosinase were removed, and then Gasteiger charges and hydrogen atoms were added to the PDB file. The docking calculations were performed by using the Lamarckian genetic algorithm (LGA) and the search parameter was set to run 100 times.

2.8. Statistical analysis

All the experiments were conducted three times unless otherwise stated. Data were expressed as the mean \pm standard deviation. One-way analysis of variance (ANOVA) was performed by utilizing Origin 8.0 and $p < 0.05$ was considered statistically significant.

3. Results and discussion

3.1. Effects of DMY and vitamins on tyrosinase activity

As shown in Fig. 1A, when the concentration of tyrosinase was kept constant, the activity of tyrosinase conspicuously decreased with increasing concentrations of DMY and kojic acid (positive control). The IC₅₀ values of DMY and kojic acid were $(3.66 \pm 0.14) \times 10^{-5}$ and $(4.64 \pm 0.37) \times 10^{-5}$ mol L⁻¹,

respectively. They exhibited a similar inhibitory capacity on tyrosinase activity. Compared with DMY, vitamins D₃ and E showed a weaker inhibition activity on tyrosinase, whereas vitamin B₆ almost had no inhibition activity against tyrosinase (Fig. 1B). At present, researchers have paid more attention to the inhibition of a single inhibitor and less to the inhibitory effects of combinations of two inhibitors. A synergistic effect means that the sum of each inhibitor alone is less than the joint inhibitory ability. If the sum of each inhibitor alone is equal to the joint inhibitory ability, it is called the additive effect. The joint effect of vitamins on the inhibition of tyrosinase by DMY was determined according to the literature.^{21,22} In the assay, the three vitamins were mixed with DMY, respectively, and then the effects of different mixtures on tyrosinase were analyzed. The relative enzymatic activity in the presence of DMY is represented as V_a . V_b denotes the relative enzymatic activity after the addition of vitamin. The relative enzymatic activity in the presence of both DMY and one vitamin was defined as V_{ab} . If the inhibitory effects on tyrosinase of DMY and one vitamin are independent, the final remnant activity fraction of tyrosinase (V_c) is equal to $V_a \times V_b$. The values of $V_{ab}-V_c$ below -0.10 were recorded as synergy (SY), the values between -0.1 and $+0.1$ were considered as additive (AD), and the values beyond $+0.10$ were regarded as subadditive (SU).⁷ As shown in Table 1, when the concentration of DMY was 1.33×10^{-5} mol L⁻¹ and the concentration of vitamin D₃ was 3.3×10^{-5} or 8.3×10^{-5} mol L⁻¹, the DMY-vitamin D₃ mixture showed a synergetic effect on the inhibition of tyrosinase. However, with increasing the concentration of vitamin D₃ from 8.3×10^{-5} to 2.00×10^{-4} mol L⁻¹, the joint effect mode was changed from synergetic to additive effects. When the concentration of vitamin D₃ was 3.3×10^{-5} , 8.3×10^{-5} or 2.00×10^{-4} mol L⁻¹ and the concentration of DMY was 4.00×10^{-5} or 9.33×10^{-5} mol L⁻¹, the DMY-vitamin D₃ system exerted an additive effect, except for a subadditive effect at DMY and vitamin D₃ concentrations of 9.33×10^{-5} and 2.00×10^{-4} mol L⁻¹. Compared to vitamin D₃, vitamins B₆, or E showed additive or subadditive effects on the inhibition of tyrosinase in the studied concentrations. These results indicated that the

addition of vitamins B₆, D₃ or E could influence the inhibition activity of tyrosinase by DMY.

3.2. Reversibility

The plots of the ν versus [tyrosinase] at different concentrations of DMY are shown in Fig. 1C. All the lines showed good linearity and passed through the origin. Furthermore, increasing concentration of DMY caused a decrease in the slope of the lines, indicating that DMY did not reduce the amount of efficient enzyme available except inhibiting tyrosinase activity. The results indicated that DMY reversibly inhibited tyrosinase activity, and there was a non-covalent intermolecular interaction between DMY and tyrosinase.^{23,24}

3.3. Inhibitory kinetics

Lineweaver-Burk double reciprocal plots were used to validate the inhibition type of DMY on the tyrosinase activity during the oxidation of L-dopa. As shown in Fig. 1D, the four lines intersected in the second quadrant with different slopes and intercepts, and the apparent K_m increased with the decreasing V_{max} , suggesting that DMY induced mixed-type inhibition on tyrosinase and may bind to both free tyrosinase and the L-dopa-tyrosinase complex.^{25,26} The values of K_i and K_{is} were calculated to be $(8.97 \pm 0.45) \times 10^{-5}$ and $(2.37 \pm 0.13) \times 10^{-4}$ mol L⁻¹ by eqn (1)–(3), respectively. It implies that DMY may tend to more easily and firmly bind to the free tyrosinase than to the DMY-tyrosinase complex since the values of K_{is} was greater than that of K_i for the oxidation of L-dopa. It was speculated that the affinity between tyrosinase and L-dopa diminished in the presence of DMY.²⁷ In addition, the secondary replots of slope and Y-intercept versus [DMY] were linearly fitted, suggesting that DMY may have a single class of inhibition sites or a single inhibition site on tyrosinase.

3.4. Fluorescence quenching of tyrosinase by DMY

As shown in Fig. 2A, tyrosinase exhibited a strong emission peak at 354 nm, while DMY showed almost no fluorescence band. With the addition of DMY, the fluorescence intensity of tyrosinase at 354 nm was gradually quenched with a red shift

Table 1 Interaction effects of DMY with vitamin B₆, vitamin D₃, or vitamin E on the inhibition of tyrosinase at various concentrations

Concentrations (mol L ⁻¹)	DMY (1.33×10^{-5} mol L ⁻¹)			DMY (4.00×10^{-5} mol L ⁻¹)			DMY (9.33×10^{-5} mol L ⁻¹)		
	Value		Interaction $V_{ab}-V_c$	Value		Interaction $V_{ab}-V_c$	Value		Interaction $V_{ab}-V_c$
	Obsd (V_{ab})	Expected (V_c)		Obsd (V_{ab})	Expected (V_c)		Obsd (V_{ab})	Expected (V_c)	
Vitamin B ₆ (1.33×10^{-4})	0.53	0.60	-0.07AD ^a	0.42	0.50	-0.08AD	0.36	0.35	0.01AD
Vitamin B ₆ (2.67×10^{-4})	0.53	0.59	-0.06AD	0.40	0.49	-0.09AD	0.36	0.34	0.02AD
Vitamin B ₆ (4.67×10^{-4})	0.42	0.50	-0.08AD	0.38	0.48	-0.10AD	0.37	0.33	0.04AD
Vitamin D ₃ (0.33×10^{-4})	0.42	0.59	-0.17SY ^b	0.41	0.47	-0.06AD	0.38	0.32	0.06AD
Vitamin D ₃ (0.83×10^{-4})	0.37	0.49	-0.12SY	0.37	0.39	-0.02AD	0.35	0.27	0.08AD
Vitamin D ₃ (2.00×10^{-4})	0.36	0.41	-0.05AD	0.35	0.33	0.02AD	0.34	0.23	0.11SU ^c
Vitamin E (0.33×10^{-4})	0.43	0.48	-0.05AD	0.39	0.38	0.01AD	0.39	0.27	0.12SU
Vitamin E (0.83×10^{-4})	0.39	0.46	-0.07AD	0.38	0.36	0.02AD	0.34	0.25	0.09AD
Vitamin E (2.00×10^{-4})	0.33	0.37	-0.04AD	0.32	0.29	0.03AD	0.31	0.21	0.10AD

^a AD means additive interaction. ^b SY means synergistic interaction. ^c SU means subadditive interaction.

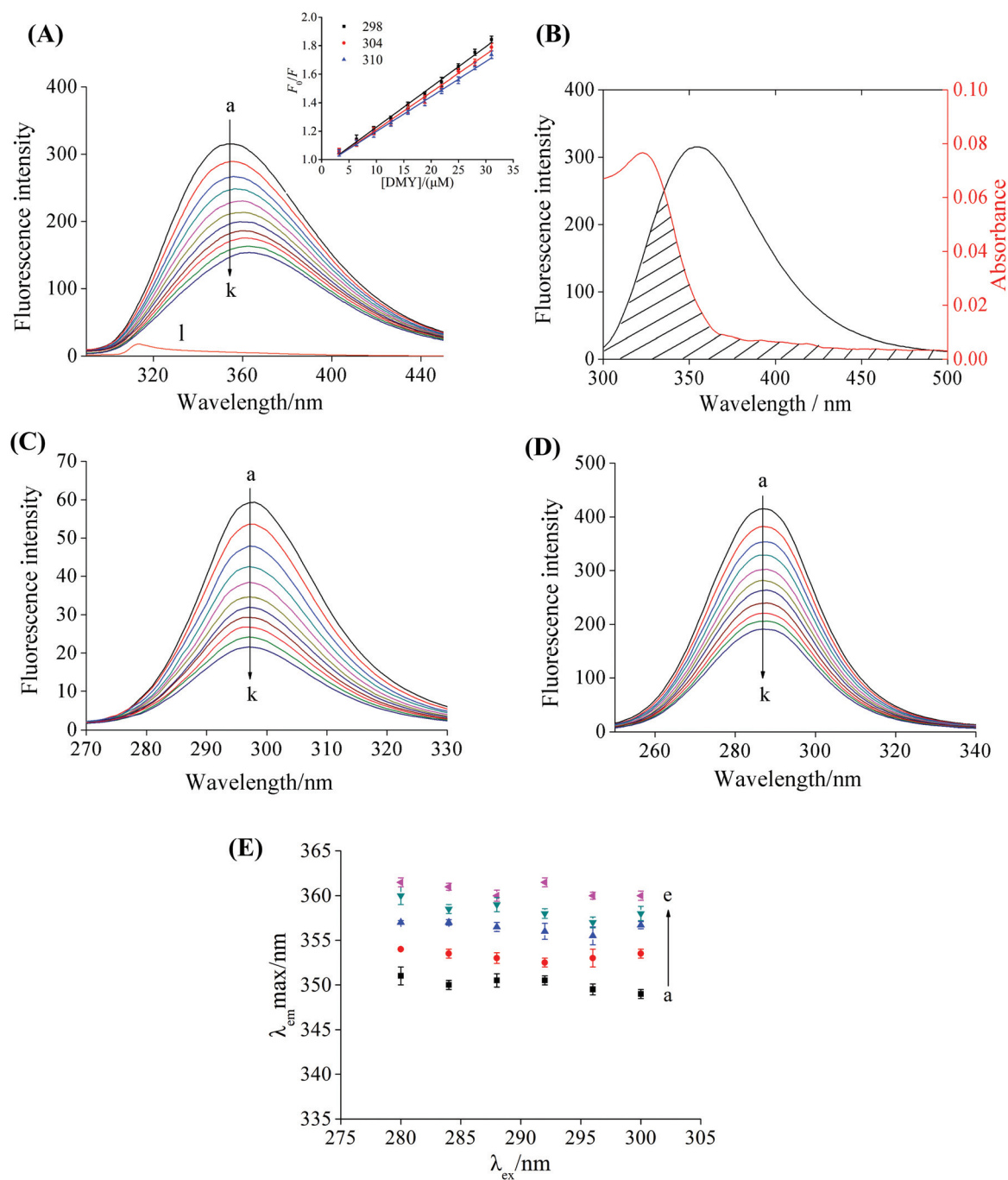


Fig. 2 (A) Fluorescence spectra of tyrosinase with different concentrations of DMY (pH 6.8, $T = 298$ K). $c(\text{tyrosinase}) = 2.4 \times 10^{-6} \text{ mol L}^{-1}$, and $c(\text{DMY}) = 0, 3.2, 6.4, 9.6, 12.8, 16.0, 19.2, 22.4, 25.6, 28.8$, and $32.0 \times 10^{-6} \text{ mol L}^{-1}$ for curves a \rightarrow k, respectively; curve l shows the emission spectra of DMY only, $c(\text{DMY}) = 3.2 \times 10^{-6} \text{ mol L}^{-1}$. The inset shows Stern–Volmer plots for the fluorescence quenching of tyrosinase by DMY at three different temperatures (298, 304, and 310 K). (B) The overlap of fluorescence spectrum of tyrosinase (black) with the absorption spectrum of DMY (red) at 298 K. $c(\text{DMY}) = c(\text{tyrosinase}) = 2.4 \times 10^{-6} \text{ mol L}^{-1}$. Synchronous fluorescence spectra of tyrosinase in the absence and presence of DMY (C) $\Delta\lambda = 15$ nm, (D) $\Delta\lambda = 60$ nm. $c(\text{tyrosinase}) = 2.4 \times 10^{-6} \text{ mol L}^{-1}$, and $c(\text{DMY}) = 0, 3.2, 6.4, 9.6, 12.8, 16.0, 19.2, 22.4, 25.6, 28.8$, and $32.0 \times 10^{-6} \text{ mol L}^{-1}$ for curves a \rightarrow k, respectively. (E) Red edge excitation curves for tyrosinase before and after addition of DMY, $c(\text{tyrosinase}) = 2.4 \times 10^{-6} \text{ mol L}^{-1}$, $c(\text{DMY}) = 0, 8.0, 16.0, 24.0, 32.0 \times 10^{-6} \text{ mol L}^{-1}$ for curves a \rightarrow e, respectively.

of the emission peak (from 354 to 363 nm). This result suggested that DMY might interact with tyrosinase and induce a conformational change of tyrosinase.

The mechanism of fluorescence quenching was usually classified as static quenching and dynamic quenching.¹⁵ In order to ascertain the fluorescence quenching mechanism of

tyrosinase caused by DMY, the fluorescence data were calculated by using the Stern–Volmer equation:²⁸

$$\frac{F_0}{F} = 1 + K_{SV}[Q] = 1 + K_q\tau_0[Q] \quad (5)$$

where F_0 and F represent the fluorescence intensities of tyrosinase in the absence and presence of DMY, respectively; K_{SV} denotes the Stern–Volmer quenching constant, which could be obtained by the linear regression of a plot of F_0/F against $[Q]$; K_q and τ_0 (10^{-8} s) are the bimolecular quenching rate constant ($K_q = K_{SV}/\tau_0$) and the average lifetime of the fluorophore in the absence of DMY, respectively; $[Q]$ is the concentration of DMY.

As shown in the inset of Fig. 2A, all the curves had a good linearity, indicating that the fluorescence quenching procedure is single type. The values of K_{SV} at 298, 304, and 310 K were in the order of magnitude of 10^4 L mol⁻¹ and showed a decreasing trend with the increase of temperature (Table 2). Moreover, the calculated K_q values (2.82×10^{12} , 2.64×10^{12} , and 2.45×10^{12} L mol⁻¹ s⁻¹ at 298, 304, and 310 K, respectively) were much greater than the maximal scatter collision quenching constant (2.0×10^{10} L mol⁻¹ s⁻¹). All these results indicated that the fluorescence quenching of tyrosinase by DMY was a static quenching process.

3.5. Binding constant and number of binding sites

For static quenching, the binding constant (K_a) and the number of binding sites (n) were determined based on the following equation:²⁹

$$\log \frac{F_0 - F}{F} = n \log K_a - n \log \frac{1}{[Q_t] - \frac{(F_0 - F)[P_t]}{F_0}} \quad (6)$$

where $[Q_t]$ and $[P_t]$ are the concentrations of DMY and tyrosinase, respectively. As shown in Table 2, the K_a values at three different temperatures (298, 304, and 310 K) were in the order of magnitude of 10^5 L mol⁻¹, indicating that a high affinity existed between DMY and tyrosinase. The values of K_a showed a decrease with an increase in the temperature, indicating that the stability of the DMY–tyrosinase complex decreased at higher temperatures. Moreover, the values of n were close to 1 at different temperatures, suggesting that there was one binding site on tyrosinase for DMY.

3.6. Thermodynamics

The thermodynamic parameters of the binding process, including enthalpy change ΔH° and entropy change ΔS° could be

used to determine the main binding forces, and their values could be obtained on the basis of the van't Hoff equation:

$$\log K_a = -\frac{\Delta H^\circ}{2.303RT} + \frac{\Delta S^\circ}{2.303R} \quad (7)$$

if the values of ΔH° do not conspicuously vary with the temperature range studied, ΔH° could be considered as a constant, and then the free energy change ΔG° could be evaluated using the following relationship:

$$\Delta G^\circ = \Delta H^\circ - T\Delta S^\circ \quad (8)$$

where R denotes the gas constant (8.314 J mol⁻¹ K⁻¹) and the temperatures are 298, 304, and 310 K. The values of ΔH° and ΔS° were calculated to be -18.45 ± 0.12 kJ mol⁻¹ and 38.25 ± 0.12 J mol⁻¹ K⁻¹ respectively by eqn (7) (Table 2). According to the Ross and Subramanian's law,³⁰ $\Delta H^\circ < 0$ and $\Delta S^\circ > 0$ represented that hydrophobic forces and hydrogen bonds played an important role in the interaction process. The negative signal for ΔG° and ΔH° means that the interaction of DMY with tyrosinase was spontaneous and exothermic.

3.7. Binding distance

In the light of the Förster's non-radiative energy transfer theory,³¹ the distance between tyrosinase and DMY could be analyzed. The quantum yield (φ) of tyrosinase can be determined by comparing the fluorescence intensity of human serum albumin (HSA) solution under the same conditions by utilizing the following equation:³²

$$\varphi = \varphi_{st} \frac{F}{F_{st}} \frac{A_{st}}{A} \quad (9)$$

where F and F_{st} denote the fluorescence intensities of tyrosinase and HSA; A and A_{st} mean the absorption of tyrosinase and HSA at an excitation wavelength of HSA; φ and φ_{st} represent the fluorescence quantum yields of tyrosinase and HSA ($\varphi_{st} = 0.13$). φ was calculated to be 0.29 by eqn (9). The efficiency of energy transfer E and the average distance r between tyrosinase and DMY can be obtained by the equations:

$$E = \frac{R_0^6}{R_0^6 + r^6} = \frac{F_0 - F}{F_0} \quad (10)$$

$$R_0^6 = 8.79 \times 10^{-25} \kappa^2 N^{-4} \varphi J \quad (11)$$

$$J = \frac{\sum F(\lambda) \varepsilon(\lambda) \lambda^4 \Delta \lambda}{\sum F(\lambda) \Delta \lambda} \quad (12)$$

Table 2 Quenching constants K_{SV} , binding constants K_a , number of binding sites n , and relative thermodynamic parameters of the interaction between DMY and tyrosinase at different temperatures

T (K)	K_{SV} ($\times 10^4$ L mol ⁻¹)	R^a	K_a ($\times 10^5$ L mol ⁻¹)	R^b	n	ΔH° (kJ mol ⁻¹)	ΔG° (kJ mol ⁻¹)	ΔS° (J mol ⁻¹ K ⁻¹)
298	2.82 ± 0.02	0.9959	1.69 ± 0.12	0.9993	0.84 ± 0.04	-18.45 ± 0.12	-29.85 ± 0.2	38.25 ± 0.12
304	2.64 ± 0.04	0.9891	1.48 ± 0.32	0.9989	0.87 ± 0.05		-30.08 ± 0.3	
310	2.45 ± 0.03	0.9931	1.27 ± 0.10	0.9965	0.86 ± 0.03		-30.31 ± 0.2	

^a R is the correlation coefficient for the K_{SV} values. ^b R is the correlation coefficient for the K_a values.

where R_0 denotes the critical distance when the transfer efficiency is 50%; F_0 and F are the same as in eqn (5); κ^2 is the orientation factor of dipole; N is the refractive index of medium; ϕ represents the fluorescence quantum yields of tyrosinase; and J is the overlap integral between the fluorescence emission spectra of tyrosinase and the absorption spectra of DMY (Fig. 2B). In this study, $\kappa^2 = 2/3$, $N = 1.336$.¹⁴ The values of the parameters were $J = 1.61 \times 10^{-14} \text{ cm}^3 \text{ L mol}^{-1}$, $R_0 = 2.11 \text{ nm}$, $E = 0.05$, and $r = 3.43 \text{ nm}$ according to eqn (10)–(12). The value of r was less than 8 nm and $0.5R_0 < r < 1.5 R_0$, suggesting that there was non-radiative energy transfer from tyrosinase to DMY. Furthermore, $r > R_0$ further supported that this fluorescence quenching is static between DMY and tyrosinase.³³

3.8. Conformational changes of tyrosinase

The conformational changes of tyrosinase with the binding of DMY were investigated by the synchronous fluorescence, Red edge excitation shift (REES), CD, and FT-IR spectroscopy. Synchronous fluorescence could offer information about the changes of tryptophan and tyrosine residues in tyrosinase

when the wavelength interval $\Delta\lambda$ was fixed at 15 and 60 nm, respectively. As shown in Fig. 2C and D, the maximum emission wavelength of both tyrosine and tryptophan residues had no discernable shift, inferring that the polarity and hydrophobicity around tryptophan and tyrosine residues in tyrosinase did not conspicuously change after addition of DMY.³⁴

REES, as a relative novel approach, was also used to evaluate motions around tryptophan residues. It is defined as a shift in the emission maximum toward a higher wavelength due to a shift in the excitation wavelength toward the red edge of the absorption band.³⁵ When the tryptophan residues have a limited ability to move and limited access to a polar solvent, the REES may occur. As shown in Fig. 2E, the maximum emission of tyrosinase did not remarkably vary with the excitation wavelength in the absence of DMY, indicating that tryptophan residues in free tyrosinase were present in a fluid micro-environment. However, the addition of DMY did not cause the occurrence of REES, suggesting that DMY did not induce the significant change of the microenvironment of tryptophan residues in tyrosinase.³⁴

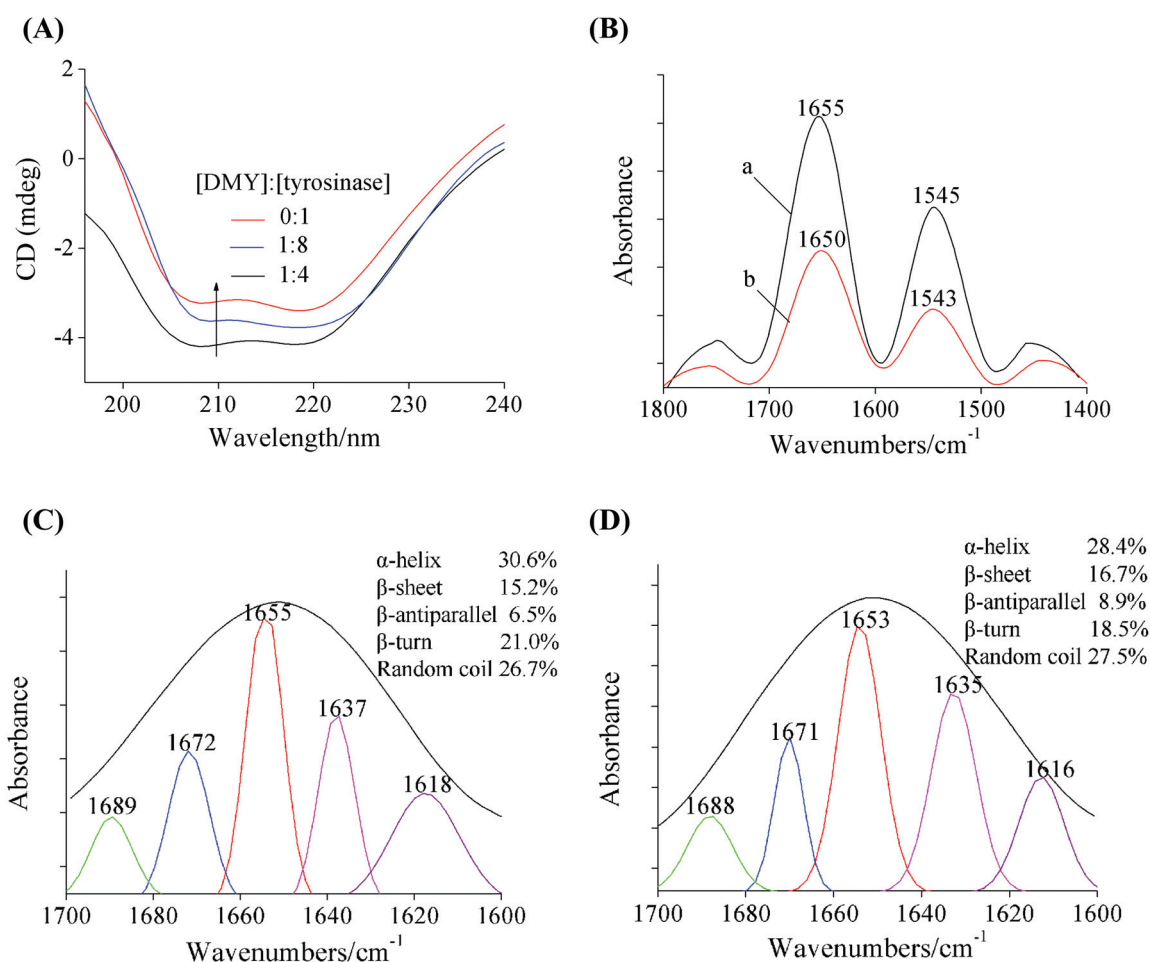


Fig. 3 (A) The CD spectra of DMY-treated tyrosinase. $c(\text{tyrosinase}) = 2.4 \times 10^{-6} \text{ mol L}^{-1}$ and the molar ratios of DMY to tyrosinase were 0 : 1, 1 : 8, and 1 : 4, respectively. (B) The FT-IR spectra of free tyrosinase (a) and difference spectra [(DMY–tyrosinase solution) – DMY solution] (b) in the region of 1800–1400 cm⁻¹. $c(\text{tyrosinase}) = 2.4 \times 10^{-6} \text{ mol L}^{-1}$, $c(\text{DMY}) = 0.6 \times 10^{-6} \text{ mol L}^{-1}$. The curve-fitted amide I region of free tyrosinase (C) and its DMY complex (D).

CD spectra measurement was used to further estimate the change of the tyrosinase secondary structure containing an α -helix, a β -sheet, a β -turn, and a random coil. As shown in Fig. 3A, the far-UV CD spectra of tyrosinase showed two negative CD bands at around 208 and 220 nm, which were characteristics of the α -helix structure of protein.³⁶ With the increasing molar ratios of DMY to tyrosinase, the intensities of the bands were decreased (shifting to zero levels). The secondary structure information of tyrosinase was obtained by SELCON3 program. When the molar ratios of DMY to tyrosinase increased from 0:1 to 1:8, 1:4, the contents of the α -helix (from 32.8% to 29.2%, 27.1%) and the β -turn (from 19.2% to 15.8%, 15.7%) decreased, while the contents of the β -sheet (from 22.3% to 25.9%, 27.8%) and the random coil (from 25.7% to 29.1%, 29.4%) increased, respectively. A similar result was reported in the interaction of apigenin with poly-

phenoloxidase.⁷ It was concluded that the binding between tyrosinase and DMY led to the unfolding of the constitutive polypeptides and decreased stability of the enzyme,³⁷ ultimately resulting in a reduction in the catalytic activity of tyrosinase.

In order to further validate the conformational changes of tyrosinase induced by DMY, FT-IR spectra were used to analyze the binding of DMY to tyrosinase. The infrared spectra of protein exhibited some amide bands, and among these amide bands, the amide I band (1700–1600 cm^{-1} , mainly C=O stretch) and amide II band (1600–1500 cm^{-1} , mainly C–N stretch coupled with a N–H bending mode) are generally used for the analysis of the chemical composition and secondary structure of proteins.³⁸ As shown in Fig. 3B, the peak position of the amide I band altered from 1655 to 1650 cm^{-1} , and the amide II band moved from 1545 to 1543 cm^{-1} upon the addition of DMY, indicating that DMY interacted with the

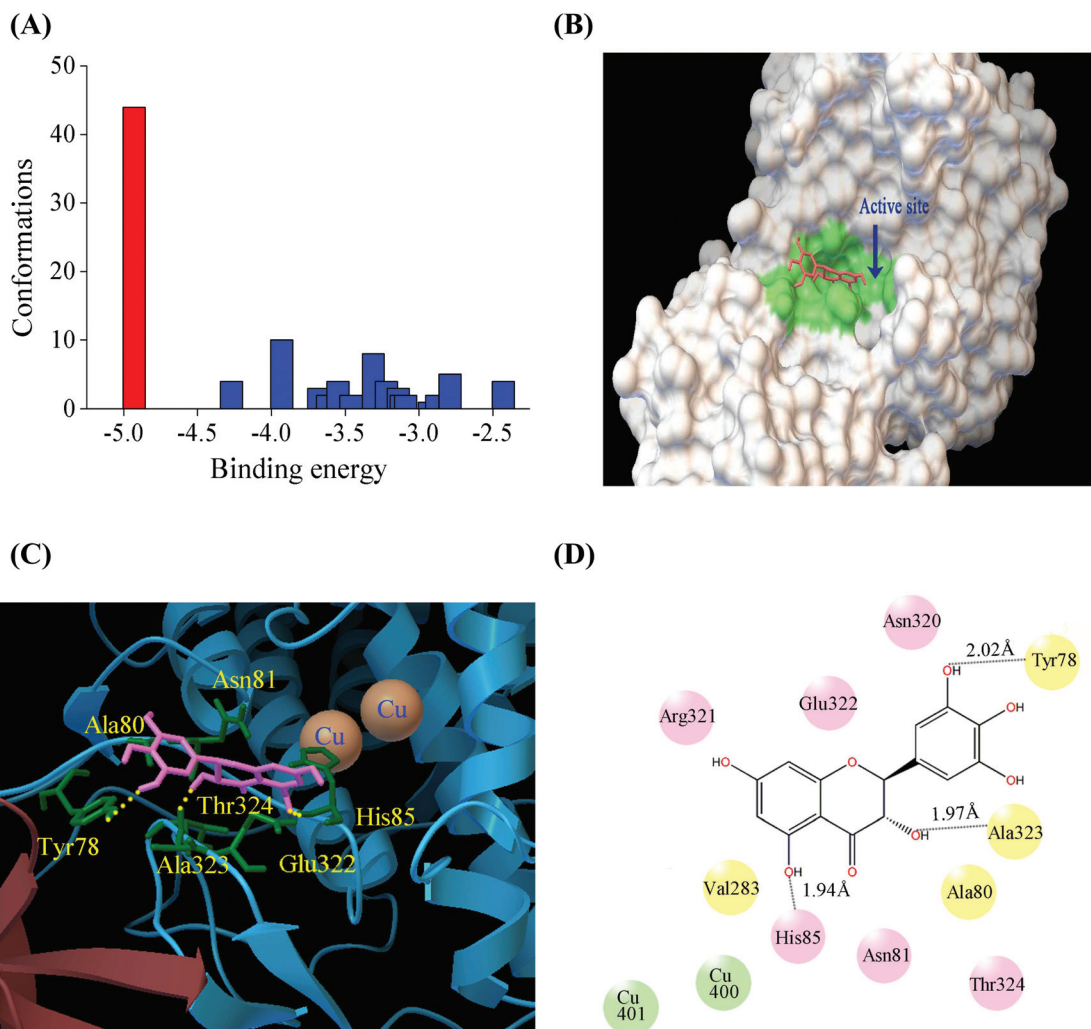


Fig. 4 (A) Cluster analyses of the AutoDock docking runs of DMY with tyrosinase. (B) Predicted binding mode of DMY docks into tyrosinase. The green parts show the hydrophobic cavity of tyrosinase. (C) The corresponding secondary structures of tyrosinase in the presence of DMY (pink carbons) are shown by a ribbon form. The light brown balls are copper atoms. The residues of tyrosinase are shown by the stick structure and the yellow dashed lines stand for hydrogen bonds. (D) Analysis of the interaction between DMY and amino acids including hydrophobic and hydrophilic residues around the active site of tyrosinase. Pink balls represent hydrophilic amino acids and yellow balls stand for hydrophobic amino acids.

C=O and C–N groups in the protein structure subunits, leading to the rearrangement of the polypeptide carbonyl hydrogen bonding pattern.³⁹ The amide I band could be divided and curve-fitted into five band ranges. The deconvoluted spectra showed that the peaks at 1655, 1672, 1689, 1637, and 1618 cm^{−1} were due to the α -helix, β -turn, β -antiparallel, random coil, and β -sheet structures, respectively (Fig. 3C). With the increasing molar ratios of DMY to tyrosinase (from 0 : 1 to 1 : 4), the position of the peaks slightly moved and the contents of the α -helix and β -turn decreased from 30.6% to 28.4% and from 21.0% to 18.5%, while the β -antiparallel, random coil, and β -sheet increased from 6.5% to 8.9%, from 26.7% to 27.5%, and from 15.2% to 16.7%, respectively (Fig. 3D). These results were in accordance with the results from CD spectra analysis, further validating that DMY may cause the change of the secondary structure of tyrosinase, resulting in the decrease of tyrosinase stability.

3.9. Molecular simulation

The crystal structure of tyrosinase includes four identical parts,⁴⁰ thus one of them was used as the crystal structure of tyrosinase for computational docking analysis.¹⁴ The cluster analysis was carried out by a root-mean-square deviation (rmsd) tolerance of 2.0 Å (Fig. 4A). Based on the energy clusters, the optimal binding mode with the lowest energy (−2.62 kcal mol^{−1}) and the most frequent locus (red histogram) was selected for further analysis. As shown in Fig. 4B, DMY was found to insert into the hydrophobic cavity of tyrosinase (green region) and is surrounded by amino acid residues Ala80, Asn81, Thr324, Tyr78, His85, Glu322, Val283, and Ala323 of tyrosinase. Among them, Ala80, Tyr78, Val283, and Ala323 are the hydrophobic amino acids (Fig. 4D). Moreover, three hydrogen bonds (yellow line) between DMY and the amino acid residues were observed (Fig. 4C), the first one was formed with the His85 residue (1.94 Å), the second one was generated with the Ala323 residue (1.97 Å), and the last one was formed with the Tyr78 residue (2.02 Å). These results suggested that the binding of DMY to tyrosinase may be driven mainly by hydrophobic interactions and hydrogen bonds, which was confirmed by the result of the above thermodynamic analysis. Therefore, we may obtain some useful information for DMY-induced inhibition to predict the binding site in the active site pocket of tyrosinase through the molecular simulation study.

4. Conclusions

In summary, DMY reversibly inhibited the activity of tyrosinase in a mixed-type manner with an IC₅₀ value of $(3.66 \pm 0.14) \times 10^{-5}$ mol L^{−1} and a K_i value of $(8.97 \pm 0.45) \times 10^{-5}$ mol L^{−1}. The dietary vitamins B₆ or E showed additive or subadditive effects with DMY on the inhibition of tyrosinase in the studied concentrations, while vitamin D₃ and DMY at the lower concentrations displayed a synergistic effect on the inhibition of tyrosinase. DMY bound spontaneously into the active cavity of

tyrosinase to form a high-affinity DMY–tyrosinase complex with one binding site, and the binding was mainly driven by hydrophobic interactions and hydrogen bonds. The binding of DMY to tyrosinase induced the rearrangement and unfolding of the constitutive polypeptides of tyrosinase with reductions in the α -helix and β -turn and increase in the β -sheet and random coil structures. The molecular docking showed that DMY inserted into the hydrophobic cavity and was surrounded by amino acid residues Ala80, Asn81, Thr324, Tyr78, His85, Glu322, Val283, and Ala323 located within the active site pocket of tyrosinase. Therefore, DMY could be a promising tyrosinase inhibitor that may inhibit tyrosinase activity by inserting into the active site of tyrosinase, occupying the catalytic center of tyrosinase to hinder entrance of the substrate and inducing conformational changes of the enzyme. This study may provide new insights into the inhibition mechanism of DMY on tyrosinase and valuable information for the functional research of DMY in the supplementary treatment of skin disorders associated with melanin deposition.

Acknowledgements

This work was financially supported by the National Natural Science Foundation of China (no. 31460422 and 21167013), the Natural Science Foundation of Jiangxi Province (20171BBB204029 and 20143ACB20006), the Objective-Oriented Project of State Key Laboratory of Food Science and Technology (SKLF-ZZA-201612), and the Postgraduate Innovation Fund of Nanchang University (CX2016213).

References

- 1 Q. X. Chen and I. Kubo, *J. Agric. Food Chem.*, 2002, **50**, 4108–4112.
- 2 W. M. Chai, M. K. Wei, R. Wang, R. G. Deng, Z. R. Zou and Y. Y. Peng, *J. Agric. Food Chem.*, 2015, **63**, 7381–7387.
- 3 Y. X. Si, Z. J. Wang, D. Park, H. Y. Chung, S. F. Wang, L. Yan, J. M. Yang, G. Y. Qian, S. J. Yin and Y. D. Park, *Int. J. Biol. Macromol.*, 2012, **50**, 257–262.
- 4 M. E. Chiari, D. M. A. Vera, S. M. Palacios and M. C. Carpinella, *Bioorg. Med. Chem.*, 2011, **19**, 3474–3482.
- 5 H. Gao, J. Nishida, S. Saito and J. Kawabata, *Molecules*, 2007, **12**, 86–97.
- 6 C. W. Zhang, Y. H. Lu, L. Tao, X. Y. Tao, X. C. Su and D. Z. Wei, *J. Enzyme Inhib. Med. Chem.*, 2007, **22**, 91–98.
- 7 Z. Q. Xiong, W. Liu, L. Zhou, L. Q. Zou and J. Chen, *Food Chem.*, 2016, **203**, 430–439.
- 8 J. M. Chen, X. J. Yu and Y. F. Huang, *Spectrochim. Acta, Part A*, 2016, **168**, 111–117.
- 9 B. G. Liu, J. Q. Du, J. Zeng, C. G. Chen and S. Y. Niu, *Eur. Food Res. Technol.*, 2009, **230**, 325–331.
- 10 X. Y. Yu, R. H. Liu, F. X. Yang, D. H. Ji, X. F. Li, J. Chen, H. W. Huang and P. G. Yi, *J. Mol. Struct.*, 2011, **985**, 407–412.

- 11 Y. Shen, A. K. Lindemeyer, C. Gonzalez, X. M. Shao, I. Spigelman, R. W. Olsen and J. Liang, *J. Neurosci.*, 2012, **32**, 390–401.
- 12 X. Liang, Y. P. Wu, J. H. Qiu, K. Zhong and H. Gao, *J. Food Sci.*, 2014, **79**, C1643–C1648.
- 13 L. Qiu, Q. H. Chen, J. X. Zhuang, X. Zhong, J. J. Zhou, Y. J. Guo and Q. X. Chen, *Food Chem.*, 2009, **112**, 609–613.
- 14 Y. J. Wang, G. W. Zhang, J. K. Yan and D. M. Gong, *Food Chem.*, 2014, **163**, 226–233.
- 15 Y. J. Wang, G. W. Zhang, J. H. Pan and D. M. Gong, *J. Agric. Food Chem.*, 2015, **63**, 526–534.
- 16 X. Peng, G. W. Zhang and L. Zeng, *Food Funct.*, 2016, **7**, 982–991.
- 17 X. Li, Z. R. Lü, W. Wang, X. P. Han, J. M. Yang, Y. D. Park, H. M. Zhou, Q. Sheng and J. Lee, *Process Biochem.*, 2015, **50**, 582–588.
- 18 Y. X. Si, S. J. Yin, D. Park, H. Y. Chung, L. Yan, Z. R. Lü, H. M. Zhou, J. M. Yang, G. Y. Qian and Y. D. Park, *Int. J. Biol. Macromol.*, 2011, **48**, 700–704.
- 19 W. Peng, F. Ding, Y. T. Jiang, Y. Sun and Y. K. Peng, *Food Funct.*, 2014, **5**, 1203–1217.
- 20 X. R. Pan, P. F. Qin, R. T. Liu and J. Wang, *J. Agric. Food Chem.*, 2011, **59**, 6650–6656.
- 21 S. B. Cai, O. Wang, M. Q. Wang, J. F. He, Y. Wang, D. Zhang, F. Zhou and B. P. Ji, *J. Agric. Food Chem.*, 2012, **60**, 7245–7251.
- 22 A. Katragkou, M. McCarthy, E. L. Alexander, C. Antachopoulos, J. Meletiadiis, M. A. Jabra-Rizk, V. Petraitis, E. Roilides and T. J. Walsh, *J. Antimicrob. Chemother.*, 2015, **70**, 470–478.
- 23 Y. Cui, G. Liang, Y. H. Hu, Y. Shi, Y. X. Cai, H. J. Gao, Q. X. Chen and Q. Wang, *J. Agric. Food Chem.*, 2015, **63**, 716–722.
- 24 Z. J. Wang, J. Lee, Y. X. Si, S. Oh, J. M. Yang, D. Shen, G. Y. Qian and S. J. Yin, *Process Biochem.*, 2013, **48**, 260–266.
- 25 Y. S. Lin, S. H. Chen, W. J. Huang, C. H. Chen, M. Y. Chien, S. Y. Lin and W. C. Hou, *Food Chem.*, 2012, **132**, 2074–2080.
- 26 H. Hridya, A. Amrita, S. Mohan, M. Gopalakrishnan, T. K. Dakshinamurthy, G. P. Doss and R. Siva, *Int. J. Biol. Macromol.*, 2016, **86**, 383–389.
- 27 X. X. Chen, Y. Shi, W. M. Chai, H. L. Feng, J. X. Zhuang and Q. X. Chen, *PLoS One*, 2014, **9**, e91809.
- 28 Z. Chen and D. D. Wu, *Sens. Actuators, B*, 2014, **192**, 83–91.
- 29 Y. Q. Wang and H. M. Zhang, *J. Agric. Food Chem.*, 2013, **61**, 11191–11200.
- 30 P. D. Ross and S. Subramanian, *Biochemistry*, 1981, **20**, 3096–3102.
- 31 L. A. Sklar, B. S. Hudson and R. D. Simoni, *Biochemistry*, 1977, **16**, 5100–5108.
- 32 S. Y. Bi, L. L. Yan, Y. Wang, B. Pang and T. J. Wang, *J. Lumin.*, 2012, **132**, 2355–2360.
- 33 F. Mehranfar, A. K. Bordbar and H. Parastar, *J. Photochem. Photobiol., B*, 2013, **127**, 100–107.
- 34 M. Maciążek-Jurczyk, A. Sułkowska and J. Równicka-Zubik, *Spectrochim. Acta, Part A*, 2016, **152**, 537–550.
- 35 A. H. C. de Oliveira, J. R. Giglio, S. H. Andrião-Escarso and R. J. Ward, *Biochem. Biophys. Res. Commun.*, 2001, **284**, 1011–1015.
- 36 B. S. Liu, X. N. Yan, S. N. Cao, B. H. Chong and Y. K. Lü, *Luminescence*, 2014, **29**, 211–218.
- 37 A. Anantharaman, H. Hemachandran, R. R. Priya, M. Sankari, M. Gopalakrishnan, N. Palanisami and R. Siva, *J. Biosci. Bioeng.*, 2016, **121**, 13–20.
- 38 H. Baltacıoğlu, A. Bayındırılı, M. Severcan and F. Severcan, *Food Chem.*, 2015, **187**, 263–269.
- 39 P. N. Naik, S. A. Chimatadar and S. T. Nandibewoor, *J. Photochem. Photobiol., B*, 2010, **100**, 147–159.
- 40 W. T. Ismaya, H. J. Rozeboom, A. Weijn, J. J. Mes, F. Fusetti, H. J. Wichers and B. W. Dijkstra, *Biochemistry*, 2011, **50**, 5477–5486.